

Electrochemical Reduction of CO₂ Catalyzed by Small Organophosphine Dendrimers Containing Palladium

Alex Miedaner, Calvin J. Curtis, Robert M. Barkley,[†] and Daniel L. DuBois^{*}

National Renewable Energy Laboratory, 1617 Cole Boulevard, Golden, Colorado 80401

Received July 21, 1994[⊗]

The sequential addition of diethyl vinylphosphonate to primary phosphines followed by reduction with lithium aluminum hydride can be used to synthesize small dendrimers containing up to 15 phosphorus atoms. A second approach uses the addition of bis((diethylphosphino)ethyl)phosphine to tetravinylsilane to produce a dendrimer containing 12 phosphorus atoms. The connectivities of these ligands are established unambiguously by ³¹P NMR spectroscopy. These dendrimers react with [Pd(CH₃CN)₄](BF₄)₂ to produce metalated dendrimers which catalyze the electrochemical reduction of CO₂ to CO. Relationships between catalytic properties and dendrimer structure are discussed.

Introduction

Dendritic or cascade molecules with ether, amine, amide, hydrocarbon, ester, quaternary phosphine, siloxane, germanium, ruthenium bipyridine, platinum bipyridine, and carborane structural units have been prepared by a number of research groups.^{1–10} Various uses for these materials have been proposed including calibrators, drug delivery vehicles, enzyme mimics, micelles, liposomes, liquid crystals, adhesives, and others. Another class of potentially interesting dendrimers are those containing tertiary phosphines. Such dendrimers raise the possibility of combining the rich catalytic chemistry of transition metal phosphine complexes with highly structured macromolecular chemistry. Our initial efforts in this area are the subject of this paper.

[†] Department of Chemistry and Biochemistry, University of Colorado, Boulder, CO 80309.

[⊗] Abstract published in *Advance ACS Abstracts*, October 15, 1994.

- (1) For a general review of this area, see: Tomalia, D. A.; Naylor, A. M.; Goddard, W. A., III. *Angew. Chem., Int. Ed. Engl.* **1990**, *29*, 138–175.
- (2) Padias, A. B.; Hall, H. K., Jr.; Tomalia, D. A.; McConnell, J. R. *J. Org. Chem.* **1987**, *52*, 5305–5312. Miller, T. M.; Neenan, T. X.; Kwock, E. W.; Stein, S. M. *J. Am. Chem. Soc.* **1993**, *115*, 356–357. Hawker, C. J.; Wooley, K. L.; Fréchet, J. M. J. *J. Am. Chem. Soc.* **1993**, *115*, 4375–4376. Padias, A.; Hall, H.; Tomalia, D. A. *Polym. Prepr. Am. Chem. Soc., Div. Polym. Chem.* **1989**, *30*, 119.
- (3) Buhleier, E.; Wehner, W.; Vögtle, F. *Synthesis* **1978**, 155–158.
- (4) Newkome, G. R.; Yao, Z.; Baker, G. R.; Gupta, V. K.; Russo, P. S.; Saunders, M. J. *J. Am. Chem. Soc.* **1986**, *108*, 849–850. Newkome, G. R.; Yao, Z.; Baker, G. R.; Gupta, V. K. *J. Org. Chem.* **1985**, *50*, 2003–2004. Tomalia, D. A.; Hall, B. M.; Hedstrand, D. M. *Macromolecules* **1987**, *20*, 1167–1169. Newkome, G. R.; Baker, G. R.; Sadao, A.; Saunders, M. J.; Russo, P. S.; Theriot, K. J.; Moorefield, C. N.; Rogers, L. E.; Miller, J. E.; Lieux, T. R.; Murray, M. E.; Phillips, B.; Pascal, L. *J. Am. Chem. Soc.* **1990**, *112*, 8458–8465. Kim, Y. H. *J. Am. Chem. Soc.* **1992**, *114*, 4947–4948.
- (5) Newkome, G. R.; Moorefield, C. N.; Baker, G. R.; Johnson, A. L.; Behera, R. K. *Angew. Chem., Int. Ed. Engl.* **1991**, *30*, 1176–1178. Newkome, G. R.; Moorefield, C. N.; Baker, G. R.; Saunders, M. J. *Ibid.* **1991**, *30*, 1178–1180.
- (6) Kwock, E. W.; Neenan, T. X.; Miller, T. M. *Chem. Mater.* **1991**, *3*, 775–777.
- (7) Rengan, K.; Engel, R. *J. Chem. Soc., Chem. Commun.* **1990**, 1084–1085.
- (8) Uchida, H.; Kabe, Y.; Yoshino, K.; Kawamata, A.; Tsumuraya, T.; Masamune, S. *J. Am. Chem. Soc.* **1990**, *112*, 7077–7079.
- (9) Bochkarev, M. N. *Metalloorg. Khim.* **1988**, *1*, 1338–41.
- (10) Serroni, S.; Denti, G.; Campagna, S.; Juris, A.; Ciano, M.; Balzani, V. *Angew. Chem., Int. Ed. Engl.* **1992**, *31*, 1493. Achar, S.; Puddephatt, R. J. *Ibid.* **1994**, *33*, 847–849. Newkome, G. R.; Moorefield, C. N.; Kieth, J. M.; Baker, G. R.; Escamilla, G. H. *Ibid.* **1994**, *33*, 666–668.

The polymerization of vinylphosphine has been reported previously.¹¹ The resulting material was not characterized, but it is likely that polydisperse organophosphine dendrimers were formed. The present work focuses on constructing small dendritic molecules of well-defined size and structure. The synthetic methodology used in this study relies heavily on recent advances in synthesizing polyphosphine ligands using either base-catalyzed or free-radical-catalyzed addition of phosphorus hydrogen bonds to activated olefins.^{12–17} Using this reaction, dendrimers containing as many as 15 phosphorus atoms have been prepared.

It has recently been shown that [Pd(triphosphine)(CH₃CN)]-(BF₄)₂ complexes will catalyze the electrochemical reduction of CO₂ to CO.¹⁴ Although these complexes are only one class of CO₂ reduction catalysts,¹⁸ the presence of triphosphine structural units in these catalysts suggested that dendrimers containing this functional unit might catalyze this reaction. In this paper, it is shown that metalation of small dendrimers containing 12 and 15 phosphorus atoms with [Pd(CH₃CN)₄](BF₄)₂ produces dendrimers exhibiting catalytic activity for electrochemical CO₂ reduction.

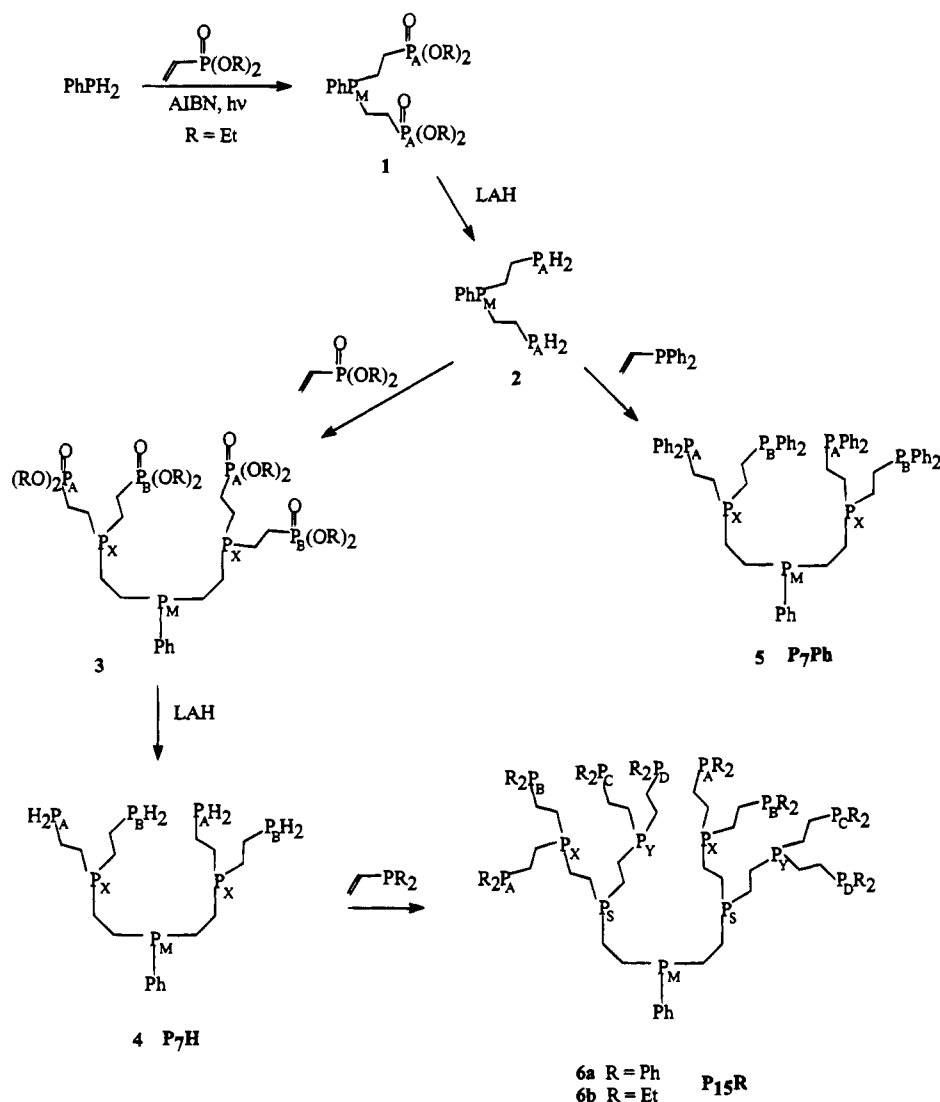
Results

Synthesis and Characterization of Phosphine Dendrimers.

The synthesis of several small dendrimers is shown in Scheme 1. The two main reactions used are the free-radical addition of diethyl vinylphosphonate to a primary phosphine and the

- (11) Lasne, M.-C.; Ripoll, J.-L.; Thuillier, A. *J. Chem. Soc., Perkin Trans. I* **1988**, 99–104. Cubioch, J. L.; Denis, J. M. *J. Organomet. Chem.* **1989**, *377*, 227–233.
- (12) King, R. B. In *Catalytic Aspects of Metal Phosphine Complexes*; Alyea, E. C., Meek, D. W., Eds.; Advances in Chemistry Series 196; American Chemical Society: Washington, DC, 1982; pp 313–323.
- (13) DuBois, D. L.; Myers, W. H.; Meek, D. W. *J. Chem. Soc., Dalton Trans.* **1975**, 1011–1015.
- (14) DuBois, D. L.; Miedaner, A.; Haltiwanger, R. C. *J. Am. Chem. Soc.* **1991**, *113*, 8753–8764.
- (15) Arpac, E.; Dahlenburg, L. *Angew. Chem., Int. Ed. Engl.* **1982**, *21*, 931–932.
- (16) Hietkamp, S.; Lebbe, T.; Spiegel, G. U.; Stelzer, O. *Z. Naturforsch.* **1987**, *42b*, 177–185. Brauer, D. J.; Lebbe, T.; Stelzer, O. *Angew. Chem., Int. Ed. Engl.* **1988**, *27*, 438–439.
- (17) Askham, F. R.; Stanley, G. G.; Marques, E. C. *J. Am. Chem. Soc.* **1985**, *107*, 7423–7431.
- (18) For reviews of electrochemical reduction of CO₂, see: *Electrochemical and Electrocatalytic Reactions of Carbon Dioxide*; Sullivan, B. P., Krist, K., Guard, H. E., Eds.; Elsevier: New York, 1993. Collin, J. P.; Sauvage, J. P. *Coord. Chem. Rev.* **1989**, *93*, 245–268.

Scheme 1



subsequent reduction of the resulting phosphonate with lithium aluminum hydride (LAH). Compounds **1** and **2** have been prepared previously using a base-catalyzed reaction.¹⁹ Compound **2** is readily purified by vacuum distillation (107 °C, 100 mmHg). Compounds **3**–**6** represent logical extensions of this reaction sequence. Compound **3** is a clear viscous oil that would not solidify or crystallize. The ¹H NMR spectrum of compound **3** (see Experimental Section) is consistent with the structure shown in Scheme 1. Most notable is the absence of resonances attributable to vinyl protons and hydrogen atoms bound to phosphorus. ³¹P NMR spectral data for this compound and other compounds prepared in this work are summarized in Table 1. The terminal phosphonate groups of **3** are diastereotopic, but the chemical shift differences are not sufficiently large to be resolved. The resonance for the phosphonate large, P_A and P_B, is a doublet due to coupling with the tertiary phosphorus atom P_X. The resonance for P_X is a doublet of triplets due to coupling to the phosphonate and phenylphosphine groups. The central phosphorus atom, P_M, is a triplet due to coupling to the tertiary phosphine atoms, P_X. The observed splitting patterns confirm the connectivity shown for **3**. The chemical shifts can be calculated using established parameters, and the good

agreement between the calculated and experimental values supports the oxidation states and substituents of the various phosphorus atoms.²⁰

Reduction of **3** with LAH produces dendrimer **4**, which contains four primary phosphine groups. This compound is a clear, air-sensitive liquid which decomposed upon attempted distillation under vacuum (~220 °C, 0.05 mmHg). The primary phosphine groups are diastereotopic, and in this case, two doublets are observed by ³¹P spectroscopy for the phosphorus atoms P_A and P_B indicating that they are sufficiently different to be resolved. The resonance for the tertiary phosphine, P_X, is a doublet of triplets arising from coupling to the primary phosphine groups and the central phosphorus atom, P_M. The P_M resonance is a triplet as expected. Again, the observed splitting patterns unambiguously establish the connectivity of the product, and the assignments are supported by the calculated chemical shifts. The primary phosphine resonance of **4** splits into a triplet when gated decoupling is used. The hydrogen atoms bound to phosphorus are observed in the ¹H NMR spectrum with the same coupling observed in the gated phosphorus spectrum (191 Hz). Similarly, the reaction of **2** with vinyl-diphenylphosphine forms dendrimer **5**. The ³¹P NMR

(19) King, R. B.; Cloyd, J. C., Jr. *J. Am. Chem. Soc.* **1975**, *97*, 46–52.
 King, R. B.; Cloyd, J. C., Jr.; Kapoor, P. N. *J. Chem. Soc., Perkin Trans. 1* **1973**, 2226–2229.

(20) Fluck, E.; Heckmann, G. *Phosphorus-31 NMR Spectroscopy in Stereochemical Analysis*; Verkade, J. G., Quin, L. D., Eds.; Methods in Stereochemical Analysis Series No. 8; VCH: Deerfield Beach, FL, 1987; pp 88–93.

Table 1. ^{31}P NMR Data for Dendrimers and Intermediates

compd	δ (calc) ^a	assgnt	<i>J</i>	
P ₃ OEt, 1	31.7 (31)	P _{A,B} (d)	53	
	-16.3 (-16)	P _M (t)		
P ₃ H, 2	-19 (-16)	P _M (t)	15	
	-128 (-128)	P _A (d)		
P ₇ OEt, 3	32.1 (31)	P _A (d)	44 (AX)	
	-16.5 (-16)	P _M (t)	22 (MX)	
	-18.3 (-20)	P _X (dt)		
P ₇ H, 4	-15.6 (-16)	P _M (t)	22 (MX)	
	-20.7 (-20)	P _X (dt)	14 (AX)	
	-128.99 (-128)	P _A (d)	14 (BX)	
	-129.03 (-128)	P _B (d)		
P ₇ Ph, 5	-12.13 (-12)	P _A (d)	24 (AX)	
	-12.17 (-12)	P _B (d)	24 (BX)	
	-17.07 (-16)	P _M (t)	21 (MX)	
	-17.67 (-20)	P _X (q)		
P ₁₅ Ph, 6a ^b	-12.39 (-12)	P _A (d)	24 (AX)	
	-12.42 (-12)	P _B (d)	24 (BX)	
	-12.44 (-12)	P _{C,D} (d)	24 (CY, DY)	
	-17.18 (-16)	P _M (t)	24 (AY)	
	-18.39 (-20)	P _S (q)	22 (MS)	
	-17.75 (-20)	P _X (q)	22 (XS)	
	-17.80 (-20)	P _Y (q)	22 (SY)	
	-17.06 (-16)	P _M (t)	19 (AX, BX, CY, DY)	
P ₁₅ E, 6b ^b	-17.98 (-20)	P _S (q)		
	-18.18 (-20)	P _X (q)	20 (MS, SX, SY)	
	-18.21 (-20)	P _Y (q)		
	-18.71 (-20)	P _A (d)		
	-18.72 (-20)	P _B (d)		
	-18.75 (-20)	P _C (d)		
	-18.79 (-20)	P _D (d)		
	-15.0 (-17)	P _C (t)	20	
	-17.9 (-20)	P _T (d)		
	[Pd ₅ (P ₁₅ Ph)(CH ₃ CN) ₅](BF ₄) ₁₀ , 8a	122.5	P _M (t)	7 (MS)
		121.1	P _X (tt)	6 (AX, BX, CY, DY)
		120.2	P _Y (tt)	
57.8		P _A	47 (SX)	
55.7		P _B	37 (SY)	
55.8		P _{C,D} (d)	341 (AB)	
62.2		P _S (m)		
119.8		P _M (t)	7 (MS)	
116.8		P _X (m)	7 (AX, BX, CY, DY)	
115.2		P _Y (m)		
[Pd ₅ P ₁₅ E(CH ₃ CN) ₅](BF ₄) ₁₀ , 8b	65.32	P _A	36 (SY)	
	62.92	P _B	45 (SX)	
	64.02	P _C	323 (AB, CD)	
	62.72	P _D		
	61.6	P _S (m)		
	117.4	P _{M'} (t)	14 (MS) ^c	
	115.3	P _X (m)	~10 (XA, XB, YC, YD)	
	115.2	P _Y (m)		
	55.1	P _A	32 (X'A, X'B, Y'C, Y'D, M'S)	
	52.9	P _B		
[Pd ₅ (P ₁₅ E)(PEt ₃) ₅](BF ₄) ₁₀ , 9	54.0	P _{C,D} (dd)	~40 (SX, SY)	
	50.10	P _S (m)	304 (AB)	
	12.15	P _{X'} (dt)	307 (MM')	
	12.10	P _{Y'} (dt)	313 (XX')	
	10.08	P _{M'} (dt)	314 (YY')	
	[Pd ₄ Si(etpE) ₄ (CH ₃ CN) ₄](BF ₄) ₈	118.8	P _C ^d (t)	6
		63.0	P _T (d)	
		118.6	P _{C'} (t)	6
	[Pd ₄ Si(etpE) ₄ (PEt ₃) ₄](BF ₄) ₈	63.1	P _{T'} (d)	
		123.1	P _C ^d	295 (CM) ^d
57.6		P _T	10 (CT)	
11.4		P _M	32 (MT)	
122.3		P _{C'}	299 (C'M')	
57.7		P _{T'}	10 (C'T')	
11.6		P _{M'}	32 (MT)	

^a All spectra were recorded in acetonitrile-*d*₃ (metal complexes) or toluene-*d*₈ (ligands) unless indicated otherwise. The chemical shifts are referenced to external H₃PO₄. Chemical shift values in parentheses were calculated according to ref 20 using aryl and alkyl group contributions of Tables 2–7. Alkyl group substituent parameters of 14 for CH₂CH₂PR₂ (R = Et, Ph, H, CH₂CH₂P) and CH₂CH₂P(O)(OEt)₂ and 17 for CH₂CH₂S are based on chemical shift values reported in refs 13–17. ^b Spectra recorded in acetone-*d*₆. ^c X', Y', and M' designate triethylphosphine ligands trans to atoms X, Y, and M, respectively, as shown in Scheme 1. ^d Letter C stands for central phosphorus atom, T for terminal phosphorus atoms, and M for the monodentate triethylphosphine ligand.

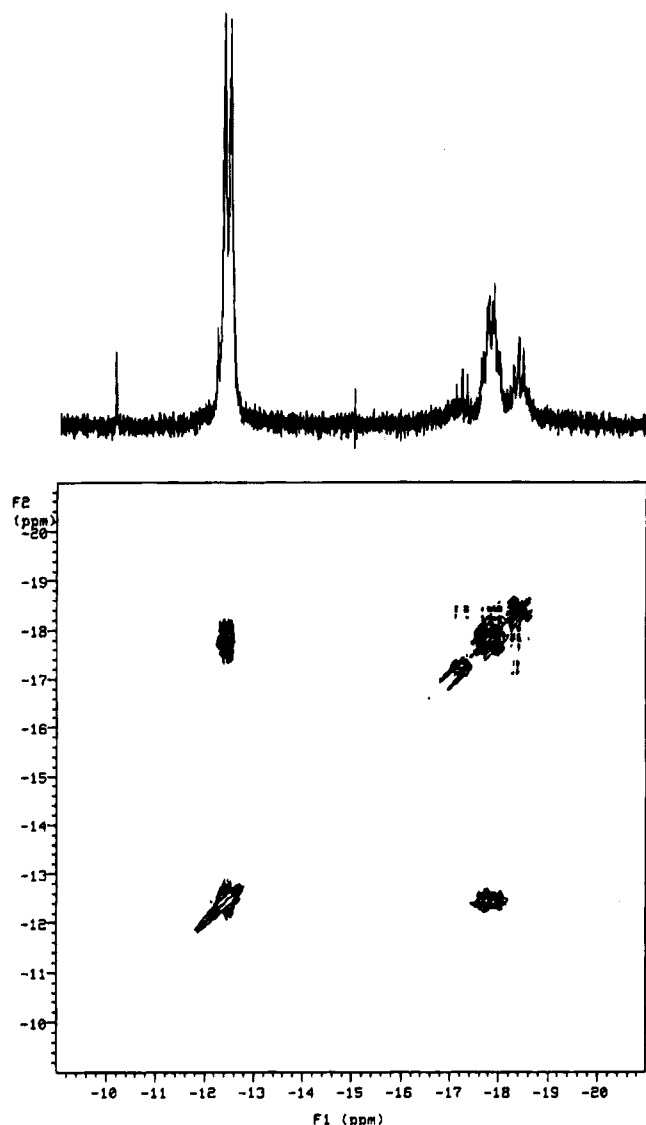


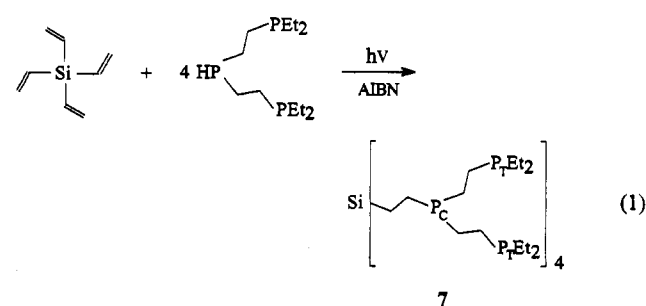
Figure 1. ³¹P NMR spectrum (202.3 MHz) of P₁₅Ph, **6a**, in acetone-*d*₆ (top). COSY ³¹P NMR spectrum of P₁₅Ph in acetone-*d*₆ (bottom).

data support a structure analogous to **3** and **4**. These data are summarized in Table 1.

Reaction of **4** with vinyl diphenylphosphine and vinyl diethylphosphine produces dendrimers **6a,b**, respectively. These dendrimers contain 15 phosphorus atoms. Compound **6a** is a white solid, while **6b** is a clear, air-sensitive oil. For dendrimers **6**, the eight terminal phosphorus atoms (P_A, P_B, P_C, and P_D) form four nonequivalent pairs. Similarly, P_X and P_Y are not equivalent. The ³¹P NMR spectrum of **6a** is shown in Figure 1. The doublets for the terminal phosphorus atoms, P_A–P_D, integrate for 8.6 phosphorus atoms. The splitting arises from coupling to either of the two phosphorus atoms P_X or P_Y. The small splitting of the doublet is attributed to the small differences in chemical shifts for P_A, P_B, P_C, and P_D. This assignment is confirmed by the off-diagonal element A,B,C,D–X,Y in the ³¹P COSY NMR spectrum shown at the bottom of Figure 1. The resonances at –17.75 and –17.80 ppm are assigned to the diastereotopic phosphorus atoms P_X and P_Y. These nuclei each couple either to P_A and P_B or P_C and P_D and a P_S nucleus as shown by the off-diagonal elements X,Y–A,B,C,D and X,Y–S of the ³¹P COSY NMR spectrum. The X,Y resonances integrate for 3.7 phosphorus atoms. The quartet resonance for P_S integrates for 1.8 phosphorus atoms and arises from the coupling to P_M, P_X, and P_Y. No coupling is observed between P_S and

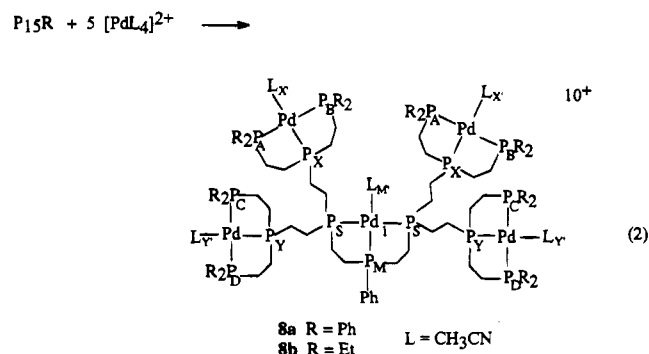
P_A–D. Finally, the triplet assigned to P_M arises from coupling to the two P_S nuclei and integrates for 1.0 phosphorus atom. The experimental and simulated ³¹P NMR spectra of **6b** are shown in Figure 2. Coupling constants and chemical shift values used for the simulation are listed in Table 1. The spin system can be reduced to eight spins for simulation by taking advantage of the mirror symmetry of **6b** and the X approximation for P_M.²¹ ³¹P COSY experiments were performed on this ligand as well and support the assignments. A positive ion fast atom bombardment (FAB) mass spectrum of **6a** exhibited a strong parent ion at *m/z* = 2168 and a fragmentation pattern consistent with loss of branches containing one and seven phosphorus atoms. A FAB spectrum of **6b** also exhibits a strong ion at *m/z* = 1400, which is one unit higher than the parent ion and is attributed to protonation of **6b** by the matrix (*m*-nitrobenzyl alcohol, MNOBA). The protonation of **6b**, but not **6a**, may be due to the greater basicity expected for **6b**. Fragmentation of **6b** is much more pronounced than for **6a**, and ions attributed to the parent ion minus fragments containing one, three, and seven phosphorus atoms are observed at *m/z* = 1282, 1106, and 753, respectively. These data provide additional support for the proposed structures.

A somewhat different approach for synthesizing phosphorus containing dendrimers is shown in reaction 1. In this reaction,



a previously constructed triphosphine ligand is attached to a tetraalkylsilane core. This reaction proceeds quantitatively to produce the small dendrimer **7**. The ³¹P NMR of the product is a doublet and a triplet as expected for the triphosphine ligand. No evidence is observed in the ³¹P and ¹H NMR spectra for residual vinyl or PH functional groups.

Palladium Complexes. The reaction of dendrimer **6b** with 5 equiv of [Pd(CH₃CN)₄](BF₄)₂ forms the metalated dendrimer **8b** as the major product (reaction 2). This dendrimer contains



five square planar metal centers, each with an inner coordination sphere composed of a triphosphine ligand and an acetonitrile

(21) Abraham, R. J. *The Analysis of High Resolution NMR Spectra*; Elsevier: New York, 1971.

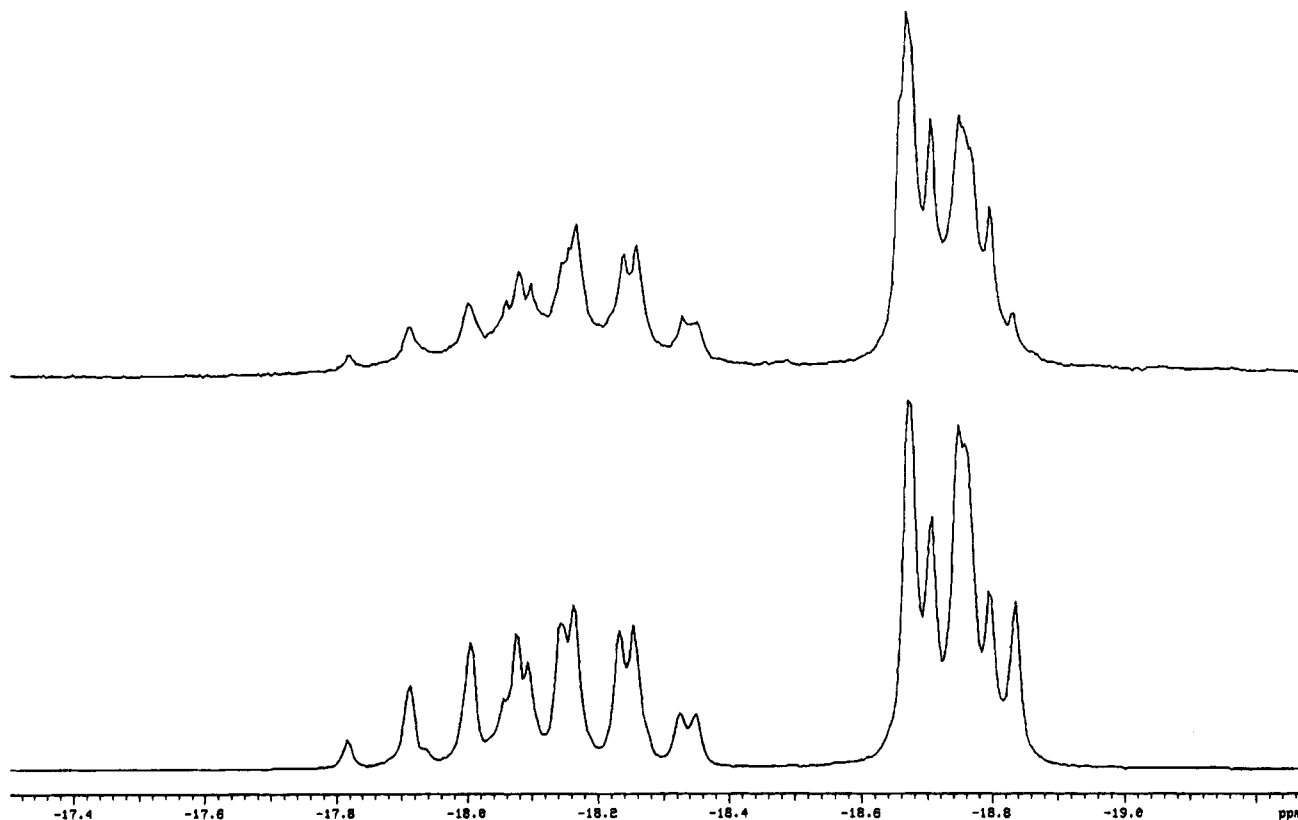
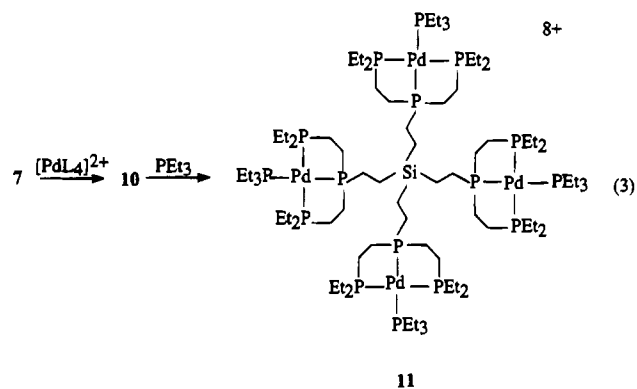


Figure 2. Experimental ^{31}P NMR spectrum (202.3 MHz) of P_{15}E (top). Simulated ^{31}P NMR spectrum of P_{15}E (bottom). The triplet resonance for phosphorus atom P_M is not shown because the eight-spin limitation of the simulation programs available results in a doublet for this nucleus. However, the remainder of the spectrum should be unaffected by this approximation.

ligand. In structures **8a,b**, the central phosphorus atoms of each triphosphine unit, P_M , P_X , and P_Y , are nonequivalent. The nonequivalence of P_X and P_Y can be attributed to the phenyl group bound to P_M . As a result of the presence of this phenyl group, the plane defined by Pd_1 , P_M , and P_S is not a mirror plane, and the two faces of the complex are different. The phosphorus atoms P_X and P_Y can lie either on the same side of the plane as the phenyl group or on the opposite side. Three resonances are observed for the three central phosphorus atoms P_M , P_X , and P_Y by ^{31}P NMR spectroscopy as shown by trace a in Figure 3. The ratio of these resonances is 1:2:2 as expected for $\text{P}_M:\text{P}_X:\text{P}_Y$. The chemical shifts for these resonances are appropriate for a coordinated tertiary phosphine incorporated in two five-membered rings. For example, the resonance for the central phosphorus atom of $[\text{Pd}(\text{etpE})(\text{CH}_3\text{CN})](\text{BF}_4)_2$ (where etpE is bis((diethylphosphino)ethyl)phenylphosphine) is a triplet at 114.1 ppm ($J = 7$ Hz).¹⁴ The terminal phosphorus atoms P_A , P_B , P_C , P_D , and P_S are nonequivalent. Two AB quartets are observed for the two sets of trans-phosphorus atoms, P_A and P_B and P_C and P_D , as seen in an expansion of this region, trace b of Figure 3. These quartets are split into doublets due to coupling to phosphorus atoms P_X and P_Y . The resonance at 61.6 ppm also exhibits a complex splitting pattern and is assigned to P_S . The ^{31}P COSY NMR spectrum shown in Figure 3 exhibits off-diagonal elements for A–B, C–D, A–X, B–X, C–Y, D–Y, S–X, S–Y, and M–S as expected on the basis of the above assignments. A proton NMR spectrum of **8b** in acetone- d_6 shows a single broad resonance at 2.2 ppm, which suggests rapid exchange between the three acetonitrile ligands coordinated to Pd_1 , Pd_2 , and Pd_3 . This resonance shifts upon adding acetonitrile indicating rapid exchange between free and coordinated acetonitrile as well. The infrared spectrum of **8b** exhibits two bands at 2293 and 2321 cm^{-1} assigned to a CN

stretching mode and a combination mode, respectively.²² Adding triethylphosphine to dendrimer **8b** replaces the acetonitrile ligands with triethylphosphine. The ^{31}P NMR spectrum of the resulting triethylphosphine-substituted dendrimer, **9**, is somewhat more complex than **8b**, but it exhibits the same general features. Spectral assignments for **9** are given in Table 1 and are supported by ^{31}P COSY experiments.

The reaction of $[\text{Pd}(\text{CH}_3\text{CN})_4](\text{BF}_4)_2$ with dendrimer **7** produces **10**, which contains four square planar palladium complexes bound to a central silicon atom (step 1 of reaction 3). The inner coordination sphere of each palladium atom



consists of a triphosphine ligand and an acetonitrile ligand, L. There are two different environments for the palladium complexes as indicated by the presence of two triplets assigned to the central phosphorus atoms of the tridentate phosphine ligands and two doublets for the terminal phosphorus atoms. This

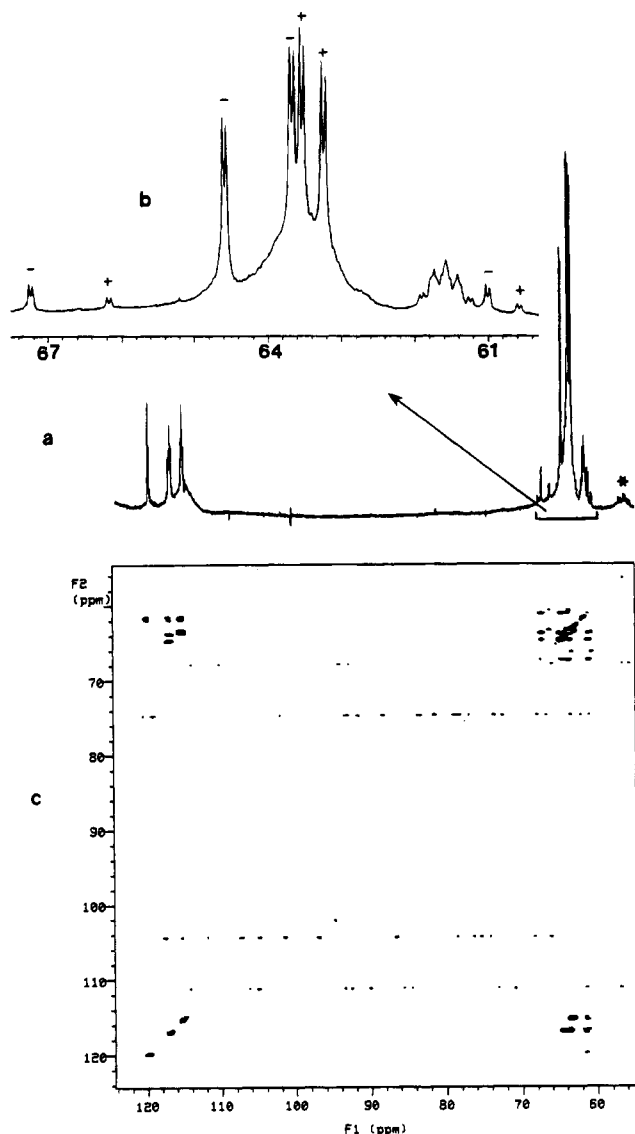


Figure 3. (a) ³¹P NMR spectrum (121.4 MHz) of [Pd₅(P₁₅E)(CH₃CN)₅](BF₄)₁₀ in acetonitrile-*d*₃. The resonances indicated by the asterisk are due to an impurity. (b) Expansion of region from 60 to 68 ppm. The transitions assigned to each of the two AB quartets are indicated by + and - signs. (c) COSY ³¹P NMR spectrum of [Pd₅P₁₅E(CH₃CN)₅](BF₄)₁₀.

nonequivalence is maintained when **10** reacts with triethylphosphine to form dendrimer **11** (step 2 of reaction 3). The ³¹P NMR spectrum of this product consists of two doublets of triplets for the central phosphorus atom, P_C and P_{C'}; a second pair of doublets of triplets for the triethylphosphine ligands; and two doublets of doublets assigned to the terminal phosphorus atoms, P_T and P_{T'}. These data again suggest two different types of environments for the palladium complexes. This nonequivalence is not observed for dendrimer **7** prior to metalation and suggests that incorporating palladium may result in restricted rotation between the square planar palladium units and nonequivalence. When complex **10** is warmed to temperatures in excess of 100 °C in dimethylformamide solutions, the two triplets and two doublets collapse to form two broad resonances indicative of a single environment. Upon lowering of the temperature to room temperature the original spectrum is observed. These results are consistent with restricted rotation for **10** and **11**.

Metalation of dendrimers **6b** and **7** forms square-planar palladium complexes coordinated by triphosphine ligands and

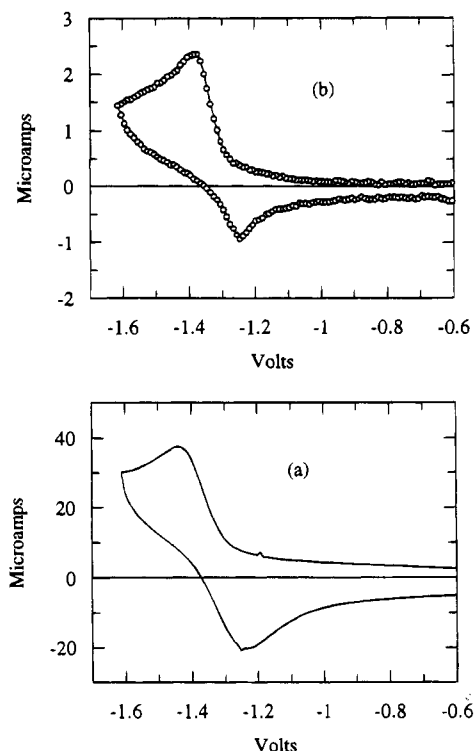


Figure 4. Cyclic voltammograms of an $\sim 0.5 \times 10^{-3}$ M dimethylformamide solution of [Pd₅P₁₅E(PEt₃)₅](BF₄)₁₀ at 10 V/s (a) and 50 mV/s (b).

a fourth ligand, either acetonitrile or triethylphosphine. The structure of dendrimer **7** is restricted in such a manner that this mode of coordination is highly favored. For dendrimers **5** and **6a,b** a number of other possible coordination modes are certainly possible. Although structures **8b** and **9** appear to be the dominant structures observed upon metalation of **6b**, the reactions of [Pd(CH₃CN)₄](BF₄)₂ with **5** and **6a** appear to be more complex. For example, the reaction of **6a** with [Pd(CH₃CN)₄](BF₄)₂ produces a product with three resonances that can be assigned to phosphorus atoms P_M, P_X, and P_Y of structure **8** and four resonances for phosphorus atoms P_A–P_D. These observations support analogous reaction products for **6a,b**. However, for **6a** these well-defined resonances are superimposed on broad resonances occurring in the same region. The broad resonances account for more than half of the total intensity. Although the broad resonances change somewhat as the temperature is varied between +50 and –80 °C, no limiting spectra are observed. Over the same temperature range, the sharp resonances are not appreciably affected. Observing exchanging and nonexchanging systems may be simply a reflection of multiple modes for binding five palladium atoms by **6a** with one of these, namely structure **8**, being more stable and less fluxional than the others. Other explanations of this behavior are also possible. The reaction of **5** with 2 equiv of [Pd(CH₃CN)₄](BF₄)₂ also appears to produce a rapidly exchanging system similar to that described for **6a**.

Electrochemical Studies of Metalated Dendrimers. Triethylphosphine Complexes. Figure 4 shows cyclic voltammograms of a dimethylformamide solution of [Pd₅(P₁₅E)(PEt₃)₅](BF₄)₁₀ at high (4 V/s) and low (50 mV/s) scan rates. At high scan rates, a quasi-reversible wave is observed at –1.34 V vs FeCp₂. The cathodic wave is diffusion-controlled, as indicated by a linear plot of *i*_p vs the square root of the scan rate for scan rates between 0.050 and 10 V/s.²³ At 4 V/s, the ratio of the anodic peak current to the cathodic peak current is 0.93, while, at 50 mV/s, this ratio is 0.47. This result is consistent with a

Table 2. Electrochemical Data for Metalated Dendrimers

compd	$E_{1/2}^a$	current efficiency		turnovers ^c	
		n^b	%		%
			CO	H ₂	
[Pd ₄ Si(etpE) ₄ (PEt ₃) ₄](BF ₄) ₈ , 11	-1.38	1.2			
[Pd ₅ (P ₁₅ E)(PEt ₃) ₅](BF ₄) ₁₀ , 9	-1.34	1.2			
[Pd ₄ Si(etpE)(CH ₃ CN) ₄](BF ₄) ₈ , 10	<-1.1	1.0	37	68	15
[Pd ₅ (P ₁₅ Ph)(CH ₃ CN) ₅](BF ₄) ₁₀ , 8a	<-1.1	1.1	14	87	1.3
[Pd ₅ (P ₁₅ E)(CH ₃ CN) ₅](BF ₄) ₁₀ , 8b	<-0.9	1.2	25	87	2

^a All potentials (V) are reported versus the ferrocene/ferrocenium couple. The values for the acetonitrile complexes reflect potentials for which significant Faradaic current flow is observed. ^b n represents the number of Faradays passed/mol of palladium at potentials approximately 100 mV negative of those shown in the $E_{1/2}$ column. ^c Current efficiencies are based on 2 Faradays/mol of H₂ or CO produced. ^d Turnovers represent the number of moles of CO produced/mol of palladium after the current has decayed to 50% of its initial value at constant CO₂ and acid concentrations.

chemical reaction following the reduction of the complex at slower scan rates. For monomeric [Pd(triphosphine)(PEt₃)]-(BF₄)₂ complexes, reversible two-electron reductions are observed at potentials comparable to those observed for [Pd₅(P₁₅E)(PEt₃)₅](BF₄)₁₀.²⁴ On this basis, the quasi-reversible reduction is assigned to two-electron reduction processes for each palladium atom. The observation that the values of ΔE_p (180 mV at 10 V/s) and $E_p - E_{p/2}$ (48 mV at 50 mV/s) are greater than the 30 mV expected for a two-electron process may be the result of slightly different potentials for the three different palladium environments, moderately slow electron-transfer kinetics, or a small negative interaction between the different palladium sites. Controlled-potential electrolysis at -1.5 V vs FeCp₂ resulted in the passing of 1.2 Faradays of current/mol of palladium. This result suggests that the ultimate oxidation state of palladium is one. Such species could readily form by comproportionation of Pd(0) sites formed by two-electron reduction processes with Pd(II) sites. Such reactions are known to form complexes with Pd-Pd bonds.¹⁴ This reaction may be promoted by the close proximity of the palladium sites in these dendrimers. The electrochemical behavior of [Pd₄Si(etpE)₄(PEt₃)₄](BF₄)₈ is similar to that of [Pd₅(P₁₅E)(PEt₃)₅](BF₄)₁₀ and is summarized in Table 2.

Acetonitrile Complexes. The cyclic voltammograms of the acetonitrile complexes [Pd₅(P₁₅Ph)(CH₃CN)₅](BF₄)₁₀, [Pd₅(P₁₅E)(CH₃CN)₅](BF₄)₁₀, and [Pd₄Si(etpE)₄(CH₃CN)₄](BF₄)₈ all exhibit broad, poorly defined waves as shown in Figure 5, trace a and inset, for [Pd₄Si(etpE)₄(CH₃CN)₄](BF₄)₈. Controlled-potential electrolysis of these complexes at approximately -1.5 V results in 1 Faraday of charge/palladium atom being passed. These results are similar to those of monomeric [Pd(triphosphine)(CH₃CN)](BF₄)₂ complexes, which are known to form Pd(I) dimers upon electrochemical reduction.¹⁴ Because [Pd(triphosphine)(CH₃CN)](BF₄)₂ complexes catalyze the electrochemical reduction of CO₂ to CO in acidic dimethylformamide solutions, these dendrimers were evaluated for their catalytic activity. Figure 5, trace b, shows a cyclic voltammogram of [Pd₄Si(etpE)₄(CH₃CN)₄](BF₄)₈ in dimethylformamide containing 0.05 M HBF₄ and 0.18 M CO₂. Trace c shows the effect of removing CO₂ by purging the solution with nitrogen. The enhanced current observed in the presence of CO₂ is attributed to the catalytic reduction of CO₂ to CO. Controlled-potential electrolysis experiments were carried out at -1.1 V on solutions containing catalyst, acid, and CO₂. For [Pd₄Si(etpE)₄(CH₃CN)₄]-

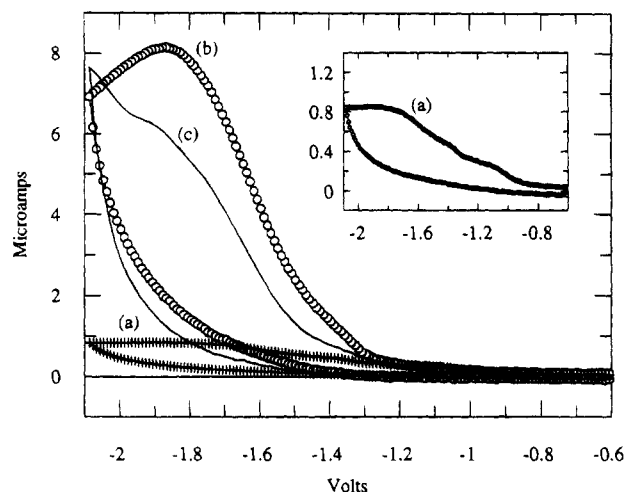


Figure 5. (a) Cyclic voltammogram of [Pd₄Si(etpE)₄(CH₃CN)₄](BF₄)₈ (1.7×10^{-3} M) in dimethylformamide under N₂ at 50 mV/s. (b) Same solution after adding HBF₄ (0.05 M) and CO₂ (0.18 M). (c) Same solution with HBF₄ (0.05 M) purged with N₂.

(BF₄)₈, 35–40% of the charge passed produced CO. In the absence of catalysts, CO₂, or acid, no CO production is observed. Similar results were obtained for the [Pd₅(P₁₅R)(CH₃CN)₅]¹⁰⁺ dendrimers; however, slightly lower current efficiencies were observed. In all cases, hydrogen production accounts for the remaining charge passed during the electrolysis experiments.

Equation 4 can be used to calculate a catalytic rate based on the current.^{14,25} Equation 4 assumes the substrate concentrations

$$\frac{i_c}{i_d} = \frac{\sigma}{0.447} \sqrt{\frac{RT}{nF}} \sqrt{\frac{kC_2^m}{v}} \quad (4)$$

are sufficiently high to ensure they are not significantly altered during the experiment. In eq 4, n is the number of electrons involved in catalyst reduction, k is the rate constant, v is the scan rate, C_2 is the concentration of substrate(s), m is an exponent corresponding to the reaction order of the substrate, and σ is a factor which depends on the mechanism. The key parameters to be measured are the catalytic current, i_c , and the diffusion current, i_d . A reliable estimate of the diffusion current is difficult to obtain directly from the acetonitrile complexes due to the poorly defined waves as shown by the inset in Figure 5. However, the current can readily be measured for the triethylphosphine analogues, Figure 4. Dividing this current by 2.83 to convert from a two-electron process to a one-electron process provides an estimate for i_d in eq 4. Using this value for i_d and the measured value of i_c , rate constants of 10 and 30 M⁻¹ s⁻¹ can be calculated for [Pd₅(P₁₅E)(CH₃CN)₅](BF₄)₁₀ and [Pd₄(SietpE)(CH₃CN)₄](BF₄)₈. These values provide an order of magnitude type of estimate for the average activity of each site in these dendrimers. Qualitatively these values are similar to those observed for discrete [Pd(triphosphine)(CH₃CN)](BF₄)₂ complexes.¹⁴

Discussion

The results presented above illustrate that the high-yield addition reaction of P-H bonds to activated olefins provides a general strategy for synthesizing small organophosphine den-

(23) Fry, A. J. *Synthetic Organic Electrochemistry*; Wiley: New York, 1989; p 31.

(24) DuBois, D. L.; Miedaner, A. *J. Am. Chem. Soc.* **1987**, *109*, 113–117.

(25) Savéant, J.-M.; Vianello, E. *Electrochim. Acta* **1965**, *10*, 905. Hammouche, M.; Lexa, D.; Momenteau, M.; Savéant, J.-M. *J. Am. Chem. Soc.* **1991**, *113*, 8455. Savéant, J.-M.; Su, K. B. *J. Electroanal. Chem.* **1985**, *196*, 1.

dimers with a variety of terminal groups. The large three-bond P–P coupling constants characteristic of ethylene linkages facilitate the characterization of these dendrimers. Both ³¹P COSY spectra and spectral simulations are important tools for establishing connectivity patterns for the larger and more complex phosphine dendrimers. The nonequivalence of various terminal and internal phosphorus atoms was observed in a number of cases.

For the dendrimer Si(etpE)₄, four discrete triphosphine functional units are separated by an intervening silicon atom and two ethylene units. As a consequence, metalation of Si(etpE)₄ with [Pd(CH₃CN)₄](BF₄)₂ yields a dendrimer containing four discrete [Pd(triphosphine)(CH₃CN)]²⁺ units. For the P₁₅R and P₇Ph dendrimers, all the phosphorus atoms are separated by simple ethylene linkages, and no separation of the dendrimer into discrete triphosphine units is inherent in their structures. Consequently, these dendrimers can coordinate to the metal as bidentate, tridentate, tetradentate, pentadentate, etc. ligands. For [Pd₅(P₁₅E)(CH₃CN)₅](BF₄)₁₀, the dominant mode of coordination appears to be discrete [Pd(triphosphine)(CH₃CN)]²⁺ complexes, although other coordination modes appear to be present as well. For the P₁₅Ph dendrimer, formation of five discrete [Pd(triphosphine)(CH₃CN)]²⁺ sites appears to constitute only a minor fraction of the possible coordination modes with the majority of the dendrimer giving broad, poorly defined resonances. The variety of coordination modes available in the P₁₅R complexes is analogous in some respects to the complexity and multitude of sites available on surfaces. The discrete sites of [Pd₄Si(etpE)₄(CH₃CN)₄](BF₄)₈ more closely approximate typical homogeneous catalysts or enzymes.

The dendritic acetonitrile complexes shown in Table 2 catalyze the electrochemical reduction of CO₂ to CO, and the rates and selectivities are similar to analogous monomeric catalysts. The order of the catalytic rates and turnover numbers for these dendrimers, [Pd₄Si(etpE)₄(CH₃CN)₄](BF₄)₈ > [Pd₅-P₁₅E(CH₃CN)₅](BF₄)₁₀ > [Pd₅P₁₅Ph(CH₃CN)₅](BF₄)₁₀, parallels the fraction of discrete [Pd(triphosphine)(CH₃CN)]²⁺ sites. These data indicate no cooperative effects occur between the palladium sites within these dendrimers. The one-electron reductions observed during bulk electrolysis experiments suggests formation of Pd(I) species with Pd–Pd bonds. Such reactions would be analogous to the Pd(I) dimers formed by reducing [Pd(triphosphine)(CH₃CN)](BF₄)₂ complexes.¹⁴ This suggests that increases in the turnover numbers may be possible if the palladium sites were well separated in dendritic catalysts. Studies to explore this possibility are in progress.

In summary, the synthesis of small polyphosphine dendrimers has been demonstrated, and palladium complexes of these dendrimers exhibit catalytic activity for the electrochemical reduction of CO₂ to CO. These results demonstrate the feasibility of performing catalytic reactions using metalated organophosphine dendrimers.

Experimental Section

Materials and Physical Methods. Reagent-grade diethyl ether, tetrahydrofuran (THF), and toluene were purified by distillation from sodium benzophenone ketyl. Acetonitrile and dichloromethane were distilled from CaH₂ under nitrogen. Reagent-grade ethanol and dimethylformamide from Burdick and Jackson were deoxygenated by purging with nitrogen prior to use. Dimethylformamide was stored in an inert-atmosphere glovebox after deoxygenation, and ethanol was stored under a positive pressure of nitrogen in a flask. Dichloromethane-*d*₂ and acetonitrile-*d*₃ were purified by vacuum transfer from CaH₂ and stored in a glovebox. Acetone-*d*₆ was dried over 4-Å molecular sieves, vacuum transferred, and stored in a glovebox. Diethyl

vinylphosphonate, diethylphosphine, diphenylphosphine, and 2,2'-azobis(2-methylpropionitrile) (AIBN) were obtained from commercial suppliers. Bis(phosphinoethyl)phenylphosphine¹⁹ and [Pd(CH₃CN)₄](BF₄)₂²⁶ were prepared by literature methods. The preparation of bis((diethylphosphino)ethyl)phosphine will be described elsewhere.

NMR spectra were obtained on a Varian Unity 300 spectrometer operating at 299.95 MHz for ¹H and 121.42 MHz for ³¹P. ³¹P NMR spectra on selected compounds were recorded on a Varian 500-MHz spectrometer operating at 202.34 MHz for ³¹P. Chemical shifts are reported in ppm relative to internal tetramethylsilane for ¹H NMR spectra and external H₃PO₄ for ³¹P NMR spectra. Infrared spectra were obtained on Nujol mulls or dichloromethane solutions using a Nicolet 510 P spectrometer. FAB mass spectra using Xe atoms at 8 keV were recorded on a VG Analytical 7070 EQ-HF tandem mass spectrometer. Samples were dissolved in *m*-nitrobenzyl alcohol (MNOBA). Elemental analyses were performed by Schwarzkopf Microanalytical Laboratories. Coulometric measurements were carried out at 25–30 °C using a Princeton Applied Research Model 173 potentiostat equipped with a Model 179 digital coulometer and a Model 175 universal programmer. The working electrode was constructed from a reticulated vitreous carbon rod with a diameter of 1 cm and a length of 2.5 cm (100 pores/in., The ElectroSynthesis Co., Inc.). The counter electrode was a W wire, and a Ag wire immersed in a 50:50 mixture of permethylferrocene/permethylferrocenium was used as the reference electrode.²⁷ The electrode compartments were separated by Vycor disks (7-mm diameter). Measurements of current efficiencies for gas production were carried out in a sealed flask (120 mL), from which gas aliquots were withdrawn for gas chromatographic analysis. Details of chromatography conditions are presented elsewhere.²⁴ In a typical experiment, a 1.0 × 10⁻³ M solution of catalyst in dimethylformamide (10.0 mL) was saturated with CO₂ by purging the solution for approximately 30 min. HBF₄ (50 μL, 9.4 M) was added via syringe and the solution electrolyzed at potentials approximately 100 mV negative of the peak potential of the first cathodic wave of the catalyst. Cyclic voltammetry and chronoamperometry experiments were carried out using a Cypress Systems computer-aided electrolysis system. The working electrode was a glassy carbon disk with a diameter of approximately 1 mm. The counter electrode was a glassy carbon rod, and the reference electrode was a Pt wire immersed in a permethylferrocene/permethylferrocenium solution. Ferrocene was used as an internal standard, and all potentials are reported vs the ferrocene/ferrocenium couple.²⁸ All solutions for cyclic voltammetry and coulometric experiments were 0.3 N NEt₄BF₄ in dimethylformamide.

Syntheses. Bis(bis(diethyl phosphonatoethyl)phosphino)ethylphenylphosphine, P₇OEt, **3**. A mixture of bis(phosphinoethyl)phenylphosphine, **2** (2.50 g, 1.0 mmol), diethyl vinylphosphonate (7.5 mL, 49 mmol), and AIBN was irradiated in a sealed Schlenk flask for 1 day. Volatile materials were removed by heating the crude product to 80 °C on a vacuum line for 16 h (9.4 g, 96%). ¹H NMR (toluene-*d*₈): Ph, 6.7–7.3 ppm (m); OCH₂CH₃, 3.6–3.7 ppm (m); CH₂P, 1.0–1.4 ppm (m); OCH₂CH₃, 0.83 ppm, t (*J* = 7 Hz).

P₇H, 4. A solution of P₇OEt (6.0 g, 6.77 mmol) in THF (50 mL) was added slowly over a 1-h period to a stirred suspension of LAH pellets (5.0 g, 0.13 mol) in THF (100 mL). The reaction mixture was stirred overnight at room temperature and then hydrolyzed slowly with water (30 mL). The white precipitate that formed was removed by filtration and extracted with two 50-mL portions of THF. The combined organic extracts were dried overnight with MgSO₄. The solution and MgSO₄ were separated by filtration, and a clear, air-sensitive liquid product was obtained (2.40 g, 75%) by removing the solvent on a vacuum line at room temperature. ¹H NMR (acetone-*d*₆): Ph, 7.35–7.6 ppm (m); PH₂, 2.73 ppm (dt, ¹J_{PH} = 191 Hz, ³J_{HH} = 6 Hz); CH₂CH₂P, 2.1–2.0 (m), 1.9–0.9 (m's).

Bis((bis(diphenylphosphino)ethyl)phosphino)ethyl]phenylphosphine, P₇Ph, 5. A mixture of **2** (1.0 g, 4.3 mmol), vinyldiphe-

(26) Sen, A.; Ta-Wang, L. *J. Am. Chem. Soc.* **1981**, *103*, 4627–4629. Hathaway, B. J.; Holah, D. G.; Underhill, A. E. *J. Chem. Soc.* **1962**, 2444–2448.

(27) Hupp, J. T. *Inorg. Chem.* **1990**, *29*, 5010–5012.

(28) Gagne, R. R.; Koval, C. A.; Lisensky, G. C. *Inorg. Chem.* **1980**, *19*, 2854–2855. Gritzner, G.; Kuta, J. *Pure Appl. Chem.* **1984**, *56*, 462–466.

nylphosphine (3.7 g, 17.4 mmol), and AIBN (0.1 g) was irradiated in a sealed Schlenk tube for 3 h and then heated to 110 °C for 30 min. Volatile materials were removed by heating the crude product to 110 °C for 8 h under vacuum. A clear tar is obtained after cooling the product to room temperature (99%). Anal. Calcd for $C_{66}H_{69}P_7$: C, 73.46; H, 6.45. Found: C, 73.68; H, 6.66. 1H NMR (toluene- d_8): Ph, 7.2 ppm (m); CH_2P , 1.0–2.0 ppm (m).

P₁₅Ph, 6a. A mixture of P₇H (0.95 g, 2 mmol), vinylidiphenylphosphine (3.85 g, 18.1 mmol), and AIBN (0.1 g) was irradiated in a Schlenk flask for 3 days. Volatile materials were removed by heating the crude product to 150 °C for 5 h on a vacuum line. An oily white solid formed on cooling to room temperature. This crude product was crystallized from diethyl ether (2.55 g, 59%). Anal. Calcd for $C_{130}H_{141}P_{15}$: C, 72.02; H, 6.55; P, 21.43. Found: C, 71.18; H, 6.63; P, 20.95. 1H NMR (toluene- d_8): Ph, 7.1 ppm (m), 7.4 ppm (m); CH_2CH_2P , 2.05–1.0 ppm (m's). FAB mass spectrum (MNOBA): parent ion, m/z = 2168; parent ion minus $P(C_6H_5)_2$, m/z = 1983; parent ion minus C_2H_4P (C_6H_5)₂, m/z = 1955; parent ion minus $P_7C_6_2H_{68}$, m/z = 1138. The mass axis was calibrated with CsI.

P₁₅E, 6b. The procedure for this dendrimer was nearly identical to that used for P₁₅Ph. The product is a clear, air-sensitive, viscous oil. 1H NMR (toluene- d_8): Ph, 7.2 and 7.6 ppm (m's); CH_2CH_2P and PC_2H_5 , 1.0–2.0 ppm (m's). FAB mass spectrum (MNOBA): (M + H), $P_{15}C_{66}H_{141}$, m/z = 1400 (43); (M + H) minus $CH_2CH_2P(C_2H_5)_2$, $P_{14}C_{60}H_{127}$, m/z = 1282 (45); $P_{12}C_{52}H_{109}$, m/z = 1106 (45); $P_8C_{36}H_{73}$, m/z = 753 (83); $P_7C_{28}H_{64}$, m/z = 617 (100); $P_3C_{12}H_{28}$, m/z = 265 (38); PC_6H_{14} , m/z = 117 (99).

Si(etpE)₄, 7. A mixture of bis((diethylphosphino)ethyl)phosphine (0.50 g, 1.9 mmol), tetravinylsilane (0.064 g, 0.47 mmol), and AIBN (10 mg) was irradiated in a Schlenk flask for 3 days. The crude product was heated to 110 °C under vacuum for 5 h to produce a clear oil (yield 0.55 g, 99%). 1H NMR (CD_3CN): $SiCH_2CH_2P$ and PCH_2CH_3 , 0.6–1.4 ppm (m's).

[Pd₅(P₁₅E)(CH₃CN)₅](BF₄)₁₀, 8b. A solution of $[Pd(CH_3CN)_4](BF_4)_2$ (0.79 g, 1.79 mmol) in acetonitrile (20 mL) was added to a solution of P₁₅E (0.50 g, 0.36 mmol) in toluene (20 mL). A precipitate formed immediately. The reaction mixture was stirred at room temperature for 3 h. The solvent was removed with a vacuum line to produce a yellow powder (1.05 g, 97%). The crude product was recrystallized from a mixture of dichloromethane and ethanol containing 5% acetonitrile by reducing the volume and cooling. Anal. Calcd for $C_{76}H_{156}N_5P_{15}Pd_5B_{10}F_{40}$: C, 30.38; H, 5.23; N, 2.33. Found: C, 29.99; H, 5.63; N, 1.74. 1H NMR spectrum (acetone- d_6): Ph, 7.2–8.3 ppm

(m's); CH_2CH_2 and C_2H_5 , 1.2–3.2 ppm (m's); CH_3CN , 2.45 ppm (s). IR (Nujol): ν_{CN} , 2293 cm^{-1} ; combination band, 2321 cm^{-1} .

[Pd₅(P₁₅Ph)(CH₃CN)₅](BF₄)₁₀, 8a. This compound was prepared in a manner analogous to $[Pd_5(P_{15}E)(CH_3CN)_5](BF_4)_{10}$. Anal. Calcd for $C_{140}H_{156}N_5B_{10}F_{40}P_{15}Pd_5$: C, 44.56; H, 4.17; N, 1.86. Found: C, 42.75; H, 4.29; N, 1.78. 1H NMR (acetone- d_6): Ph, 7.4–8.2 ppm (m's); CH_2CH_2P , 1.8–3.8 (m's); CH_3CN , 2.19 ppm (broad s). IR (Nujol): ν_{CN} , 2292 cm^{-1} ; combination band, 2321 cm^{-1} .

[Pd₅(P₁₅E)(PEt₃)₅](BF₄)₁₀, 9. Triethylphosphine (0.30 mL, 2.05 mmol) was added to a solution of $[Pd_5(P_{15}E)(CH_3CN)_5](BF_4)_{10}$ (0.5 g, 0.167 mmol) in acetonitrile (30 mL). The reaction mixture was stirred for 2 h, and the solvent was removed. The precipitate was collected by filtration and recrystallized from a mixture of acetonitrile and ethanol (yield 0.3 g, 40%). Anal. Calcd for $C_{96}H_{215}P_{20}Pd_5B_{10}F_{40}$: C, 34.02; H, 6.39; P, 18.28; Pd, 15.70. Found: C, 34.04; H, 6.13; P, 18.50; Pd, 15.94. 1H NMR (acetonitrile- d_3): Ph, 6.8–8.0 ppm (m's); CH_2CH_2P and PCH_2CH_3 , 1.0–3.0 ppm (m's).

[Pd₄Si(etpE)₄(CH₃CN)₄](BF₄)₈, 10. $[Pd(CH_3CN)_4](BF_4)_2$ (0.83 g, 1.9 mmol) was added to a mixture of Si(etpE)₄ (0.55 g, 0.47 mmol) in acetonitrile (50 mL). The reaction mixture was heated overnight at 70 °C. The solvent was removed on a vacuum line to produce a yellow powder (1.05 g, 89%). This product was recrystallized from a solution of dichloromethane and ethanol containing 5% acetonitrile. Anal. Calcd for $C_{64}H_{140}N_4Pd_4P_{12}B_8F_{32}Si$: C, 30.92; H, 5.68; N, 2.25. Found: C, 31.90; H, 6.04; N, 2.60. 1H NMR spectrum (acetone- d_6): $SiCH_2CH_2P$ and PCH_2CH_3 , 1.2–3.0 ppm (m's); CH_3CN , 2.49 ppm (s). IR (Nujol): ν_{CN} , 2294 cm^{-1} ; combination band, 2332 cm^{-1} .

[Pd₄Si(etpE)₄(PEt₃)₄](BF₄)₈, 11. Triethylphosphine (0.048 g, 0.4 mmol) was added to a solution of $[Pd_4Si(etpE)_4(CH_3CN)_4](BF_4)_8$ (0.30 g, 0.1 mmol) in acetonitrile (50 mL). The reaction mixture was stirred at room temperature for 1 h, and then the solvent was removed on a vacuum line. The yellow solid that resulted was crystallized from a mixture of dichloromethane and ethanol (yield 0.20 g, 72%). Anal. Calcd for $C_{80}H_{188}B_8F_{32}P_{16}Pd_4Si$: C, 34.48; H, 6.78; P, 17.75. Found: C, 34.19; H, 6.48; P, 16.64. 1H NMR spectrum (CD_3CN): $SiCH_2CH_2P$ and PCH_2CH_3 , 1.0–3.0 ppm (m's).

Acknowledgment. This work was supported by the United States Department of Energy, Office of Basic Energy Sciences, Chemical Sciences Division, and by the Director's Development Fund of the National Renewable Energy Laboratory. Martin Ashley's assistance in obtaining high-field ^{31}P NMR spectra is also gratefully acknowledged.